Specific features of the thermodynamics of activation in the $LaNi_5$—H_2 and $CeNi_5$—H_2 systems

N. A. Yakovleva, S. N. Klyamkin, O. A. Veremeeva, and A. A. Tsikhotskaya*

Department of Chemistry, M. V. Lomonosov Moscow State University, 1 Leninskie Gory, 119992 Moscow, Russian Federation. E-mail: yana@highp.chem.msu.ru

Using heat conducting Tian—Calvet calorimetry and volumetric measurements, the first hydrogen absorption—desorption cycles in the $LaNi_5$—H_2 and $CeNi_5$—H_2 systems were studied. The pressure—composition isotherms were plotted, the equilibrium pressures of hydrogen along the absorption and desorption branches and in the region of hysteresis for different activation steps were determined, and the enthalpies of phase transitions $\alpha \rightarrow \beta$ and $\beta \rightarrow \alpha$ were calculated. The profiles of the heat evolution curves were analyzed. It was concluded that the mechanism of the reactions studied changes upon activation.

Key words: intermetallides, hydrides, calorimetry, phase diagrams, hysteresis, activation.

Due to the ability to irreversibly absorb hydrogen in wide pressure and temperatures ranges, intermetallic compounds (IMC) are promising materials for hydrogen accumulation and storage, they can also be used to manufacture metal hydride electrochemical current sources, to extract hydrogen from hydrogen-containing industrial gases, and prepare novel magnetic materials.

To use hydrides of IMC for practical purposes, one needs information on the thermodynamics and mechanism of hydrogen absorption and desorption, which depend substantially on the number of cycles.

The so-called activation process, *viz.*, the behavior of a metal hydride system during the first three—ten cycles, is of special interest. However, the majority of publications deals with the properties of already activated IMC, *i.e.*, with materials preliminarily subjected to several hydrogenation—dehydrogenation cycles to achieve stable hydrogen-sorption characteristics.

The equilibrium pressure, concentration boundaries of the phase regions, and hysteresis factor change considerably between the first and subsequent cycle for the IMC—H_2 systems. In the first cycle, absorption involves a long induction period and, hence, equilibration in the IMC—hydrogen system also requires a significant time. Subsequent absorption—desorption cycles are accompanied by the fast absorption of hydrogen almost without an induction effect.[1—5]

The absorption pressure in the plateau region decreases sharply on going from the first to second cycle, and the desorption pressure changes insignificantly.[1—3] The authors relate this phenomenon to a considerable increase in the metallic matrix volume and the appearance of many defects and microstrains. Indeed, this is in the first cycle where the starting intermetallide is spontaneously crushed (hydride dispersion) and a new microstructure corresponding to the activated state is formed. During cyclic operations including hydrogen absorption—desorption, the particle size of $LaNi_5$ decreases from 150—300 μm in the initial state to 5—25 μm in the fifth cycle.[3] In the first cycle of hydrogen absorption—desorption, the size of coherent scattering (crystallite) regions shortens sharply, whereas the level of microstrains in the crystalline lattice increases.[6]

Thus, the mechanism of hydrogen absorption in the first cycle differs substantially from those in the subsequent cycles. Transformations occurred in the solid phase require additional energy expenses, which should affect the thermodynamic parameters of hydride formation.

However, published data on the thermodynamic regularities of the activation process are unavailable up to recently, and even estimated values of enthalpy and entropy changes in the first cycle of hydrogen absorption by nonactivated intermetallides are absent. In this work, we studied the first cycles of hydrogen absorption—desorption by intermetallides $LaNi_5$ and $CeNi_5$ using the construction of "pressure—composition" isotherms and direct calorimetric measurements.

Experimental

The starting intermetallides were prepared by melting a blend of high-purity metals (La, 99.8%; Ce, 99.8%; and Ni, 99.96%) in an electric-arc furnace with an inexpensive electrode under a purified argon pressure. To achieve homogenization, the alloys were remelted three times. The elemental composition of the resulting intermetallides was determined by inductively-coupled

Published in Russian in *Izvestiya Akademii Nauk. Seriya Khimicheskaya,* No. 1, pp. 134—139, January, 2005.

1066-5285/05/5401-0135

plasma atomic emission spectroscopy. The phase composition of the prepared samples was determined by X-ray diffraction analysis.

An experimental setup for calorimetric studies at low pressures (to 6 MPa) consisted of a system of dosed gas supply connected with a Tian—Calvet calorimeter. The setup and procedure have previously been described in detail.[7—9]

During experiments, quantities of gaseous hydrogen (0.0002—0.0003 mol) were introduced into a cell of the calorimeter containing 0.7—1.5 g of an intermetallide, and simultaneously the heat effect of the reaction was monitored as a function of the time and amount of reacted hydrogen. The composition of the hydride phase that formed was determined as H/IMC, *i.e.*, the number of hydrogen atoms per formula unit of the intermetallide. A new gas portion was not given until the instrument signal returned to the zero line. Special-purity grade hydrogen with the admixture content $\leq 10^{-5}$ vol.%, which was obtained by desorption from the $LaNi_5$-based hydride phase at 353 K, was used for hydrogenation. The partial molar enthalpies of absorption (desorption) ΔH were determined from the heat effect of the reaction

$$\alpha\text{-}LaNi_5H_x + 0.5y\,H_2 \rightleftharpoons \beta\text{-}LaNi_5H_{x+y}.$$

The measurement error was expressed as a square-mean error of the average result $\sigma^2 = \Sigma\Delta^2/n(n-1)$, where Δ is the deviation of the result from the average value, and n is the number of measurements.

The use of the differential scheme of a calorimeter made it possible to exclude corrections to the heat effect related to the introduction of hydrogen to the system and to a change in the external conditions for a prolong experiment.

A unique procedure[10] of precise P—V—T measurements in the hydrogen pressure range below 200 MPa and at temperatures from 195 to 673 K was used to study the thermodynamics of processes in the system with a high equilibrium pressure. The amount of absorbed hydrogen was determined from a pressure change in the system and calculated by the equation of state of strongly compressed hydrogen.[11] To calculate the thermodynamic parameters of formation and decomposition of the hydride phases by P—V—T, we used the fugacity of hydrogen corresponding to the equilibrium pressures in the plateau region in the isotherms and taking into account the deviation from ideality for hydrogen at high pressures. The ΔH and ΔS values of the corresponding reactions were determined by the Van´t Hoff equation from analysis of the $\ln(f)—1/T$ plots.

Results and Discussion

$LaNi_5$—H_2 system

The isotherms in the pressure—composition coordinates for the first and tenth hydrogen absorption—desorption cycles in the $LaNi_5$—H_2 system were plotted using results of volumetric measurements (Fig. 1). The isotherms of the first absorption cycles are characterized by a steep slope of the plateau, which almost disappears with the further cycling.

As can be seen from the data in Table 1, the equilibrium absorption pressure is by 5—6 times higher than

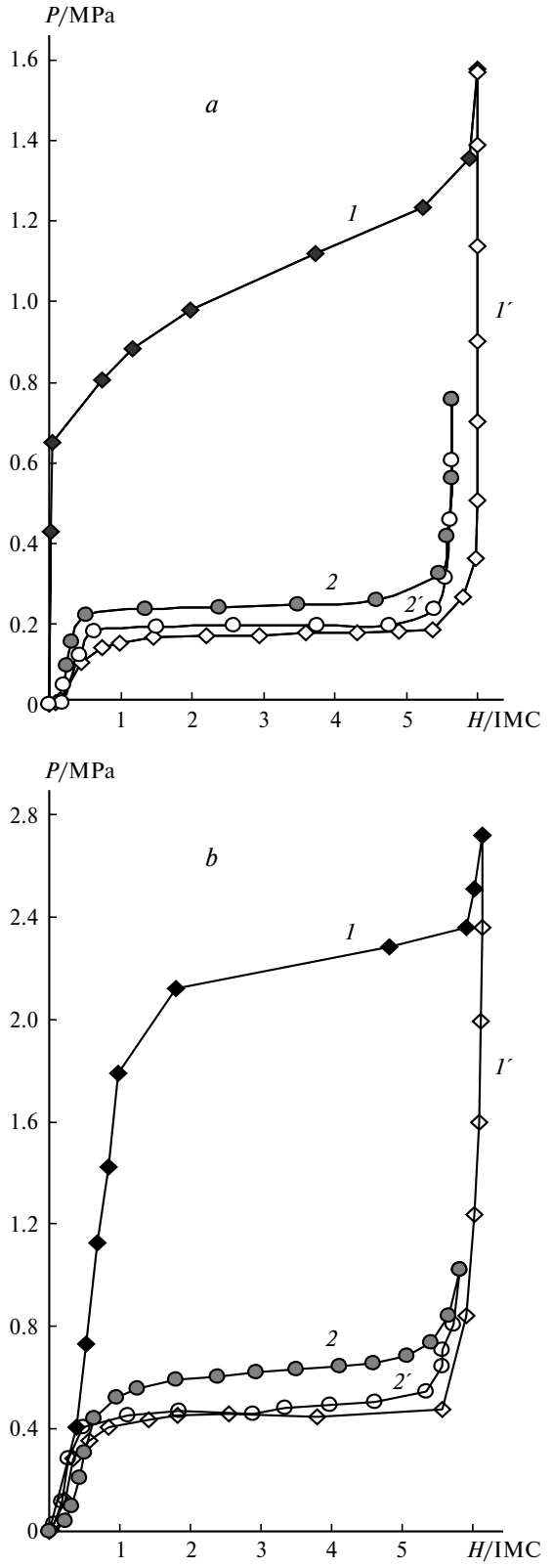

Fig. 1. Hydrogen absorption (*1*, *2*) and desorption (*1′*, *2′*) isotherms in the $LaNi_5$—H_2 system at 308 (*a*) and 328 K (*b*); *1*, *1′*, 1st cycle and *2*, *2′*, 10th cycle.

Table 1. Equilibrium pressures and hysteresis factors in the $LaNi_5$—H_2 system

T/K	Cycle	p_{abs}*	p_{des}*	$RT\ln(p_{abs}/p_{des})$ /kJ (mol^{-1} H_2)
		MPa		
308	1	1.05	0.17	4.7
	2	0.38	0.19	1.8
	3	0.28	0.19	1.0
	10	0.24	0.19	0.6
328	1	2.12	0.45	4.2
	2	0.65	0.46	0.9
	6	0.60	0.46	0.7
	10	0.59	0.46	0.7

* The equilibrium pressure of absorption—desorption is presented for H/IMC = 3.

the desorption pressure, resulting in a considerable hysteresis. The size of the hysteresis loop expressed by the $RT\ln(p_{abs}/p_{des})$ ratio decreases sharply on going from the first to second cycle and achieves a reproducible value only to the tenth cycle (see Table 1). This change is caused, first, by a decrease in the absorption pressure, while the equilibrium desorption pressure remains almost unchanged during cycling.

An insignificant temperature increase (from 308 to 328 K) noticeably affects the change in the parameters of the system during activation (*cf.* data in Fig. 1). Already in the first cycle the size of the hysteresis loop decreases, the decrease from the first to second cycle is drastic, while the further changes, on the contrary, are less pronounced.

The average partial molar enthalpies of the phase transitions $\alpha \rightarrow \beta$ and $\beta \rightarrow \alpha$ (with the corresponding plateau in the absorption and desorption isotherms, respectively) for the first hydrogenation—dehydrogenation cycles were obtained by differential heat conducting Tian—Calvet microcalorimetry (Table 2).

The average partial molar enthalpies found for the $\alpha \rightarrow \beta$ phase transition increase (by the absolute value) with an increase in the cycle number, which agrees with the general character of the change in the equilibrium pressures in the plateau range of the isotherms. In all cycles, the average partial molar enthalpy of the inverse reaction $\beta \rightarrow \alpha$ remains unchanged within the deviation from the averaged result. In the case of the first absorption, a high error of determination of the average enthalpy related, probably, to a strong nonequilibrium state of the process.

Table 2. Thermodynamic parameters of hydrogenation in the $LaNi_5$—H_2 system

T/K	Cycle	ΔH_{abs}	ΔH_{des}
		kJ (mol^{-1} H_2)	
308	1	−19.0±5.0	34.3±0.8
	2	−27.8±1.7	34.2±0.4
	3	−33.7±0.9	32.8±1.0
	10	−32.6±0.6	32.9±0.6
328	1	−25.0±2.0	30.7±0.6
	2	−32.1±0.8	31.2±0.6
	6	−32.1±0.8	31.4±0.5
	10	−31.7±0.8	31.8±0.6

The data in Table 2 confirm the temperature effect on the thermodynamics of the activation process. The temperature increase from 308 to 328 K favors the equilibriation of the system, which is manifested as a decrease in the error of determination of ΔH. In addition, the parameters of the first cycle become closer to the values characteristic of the completely activated state.

Curves of heat evolution are very informative for understanding of the activation mechanism. These plots of the thermal power *vs.* time duration obtained during calorimetric experiments are schematically presented in Fig. 2 for different regions of the pressure—composition isotherms.

The uptake of the first portion of hydrogen in the α-region for activated $LaNi_5$ (*i.e.*, after the 10th cycle) begins immediately, without an induction effect (see Fig. 2, *a*, curve *1*). The maximum heat release is observed during the first 10—15 min, and the reaction time (the time necessary for the experimental curve to return to the zero line) is 40—60 min.

When the initial hydrogen absorption in the region of an α-solution by nonactivated $LaNi_5$ occurs, the first hydrogen portion is consumed with a remarkable induction

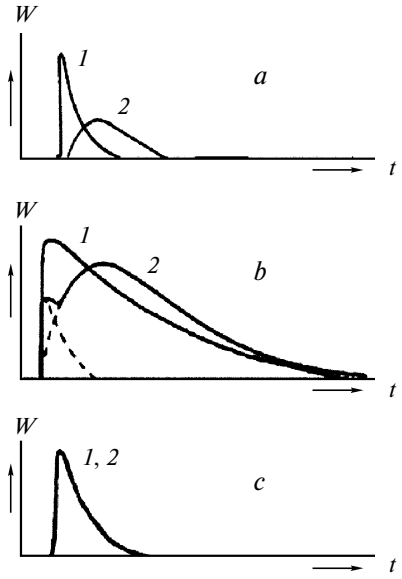

Fig. 2. Heat evolution curves for the activated (*1*) and nonactivated (*2*) IMC: *a*, region of the solid α-solution; *b*, region of the $\alpha \rightarrow \beta$ phase transition; and *c*, solution of hydrogen in β-hydride.

period (from 15 to 30 min). As compared to a similar peak for the activated IMC, the peak intensity decreases, and the peak becomes more diffuse (see Fig. 2, *a*, curve *2*). The reaction time is 15—16 h.

In the region of the $\alpha \rightarrow \beta$ phase transition for the activated alloy (see Fig. 2, *b*, curve *1*), the maximum heat evolution is observed for the first 20—30 min after the reaction onset. Then the heat evolution gradually decreases, and equilibration was finally achieved within 3—4 h.

The pronounced splitting of the maximum in the two-phase region of the heat release curves of the nonactivated IMC (see Fig. 2, *b*, curve *2*) was observed for the first time in the first cycle.

The first maximum corresponds to a higher reaction rate. During this time (15 min), 20—25% hydrogen is absorbed, which corresponds to 5% of the overall heat release. The second maximum corresponds to the absorption of 75—80% hydrogen and is characterized by a considerable (95%) heat evolution. The smoother curve indicates a lower reaction rate. Equilibration takes approximately 1 day.

For activated $LaNi_5$, hydrogen dissolution in β-hydride resembles that in the α-region (see Fig. 2, *c*, curve *1*). The character of the heat evolution curves for hydrogen dissolution in β-hydride in the first cycle is identical to the same process for activated $LaNi_5$ (see Fig. 2, *c*, curve *2*).

Let us consider the mechanism of interaction in the intermetallide—hydrogen system to interpret the effects observed above.[12,13] This heterogeneous transformation consists of several consecutive steps: the transport of gaseous hydrogen to the solid phase surface, dissociative chemosorption of hydrogen on the surface, and diffusion of hydrogen through the bulk solid phase to form a solid solution. When some limiting hydrogen concentration is achieved in the solid solution, the formation and nucleation of the hydride phase occur. As compared to the activated phase, the initial intermetallide phase is characterized by a much smaller specific surface, a higher concentration of surface defects, and, as a consequence, a smaller number of active sites available for chemosorption.[3,4] Correspondingly, at the initial step the nonactivated phase exhibits a lower rate of hydrogenation resulting in the formation of a solid α-solution (see Fig. 2, *a*).

In the two-phase α+β-region of the phase diagram, hydrogen absorption is more complex and includes an additional step of nuclei formation and growth of a new phase. The effect of maximum splitting in the heat release curves has previously[7] been observed for the $LaNi_5$—H_2 system when ultrasmall weighed samples (0.05 g) and a DAK-1 high-sensitivity microcalorimeter were used. The authors[7] attributed this effect to the ordering of the hydrogen sublattice in the phase formed by the solid α-solution. In our opinion, the strong maximum splitting in the case of the nonactivated system can be associated with a strong inhibition of nucleation of β-hydride caused by a large size of the solid phase crystallites and a low concentration of defects in this phase. As a result, an α-solution can be supersaturated at the initial moment, and the time shift of the intrinsic phase transition can occur that proceeds similarly to crystallization from an supersaturated solution, for instance, similarly to precipitation of salt from water. This interpretation seems valid because of a difference in the specific (per mole of absorbed hydrogen) heat release in the regions of the first and second maxima (see Fig. 2, *b*).

The heat effect of solid solution formation in the IMC—hydrogen systems decreases sharply with an increase in the hydrogen concentration, whereas the enthalpy of the $\alpha \rightarrow \beta$ transition remains virtually unchanged in the whole two-phase region.[7,14,15] Therefore, a relatively high hydrogen absorption in the region of oversaturated solution should be accompanied by an insignificant heat evolution, which was experimentally observed (see Fig. 2).

At the end of the $\alpha \rightarrow \beta$ phase transition, the specific expansion of the crystalline lattice achieved the maximum extent, a highly imperfect and ultradispersed microstructure is formed, and the intermetallic matrix becomes almost completely activated. The mechanism of further hydrogen dissolution in β-hydride is similar to that observed for the system at the subsequent absorption—desorption cycles.

$CeNi_5$—H_2 system

The general character of the behavior of the $CeNi_5$—H_2 system is similar to that described for $LaNi_5$. The first cycle is characterized by a strongly overestimated value of the pressure of the plateau region of the absorption isotherm and a high hysteresis (Fig. 3). A specific feature of this system is a substantially lower change in the hysteresis loop during activation. In the case of $LaNi_5$, the hysteresis factor decreases from the first to tenth cycle by 7—8 times, whereas for $CeNi_5$ it is only halved, *i.e.*, from 7.7 to 3.3 kJ (mol^{-1} H_2).

To estimate the thermodynamic parameters of hydride phase formation and decomposition in the nonactivated $CeNi_5$—H_2 system, we plotted the hydrogen absorption and desorption isotherms for the first cycle at different temperatures (273, 295, 323, and 343 K, Fig. 4). The temperature plot of the equilibrium fugacities of hydrogen corresponding to the middle region of the plateau is linear in the $\ln(f)$—$1/T$ coordinates and that allowed us to use the Van´t Hoff equation and calculate the standard change in enthalpy of the $\alpha \rightarrow \beta$ phase transition. The data for the first and third cycles of hydrogen absorption—desorption in $CeNi_5$ are presented in Table 3. It has

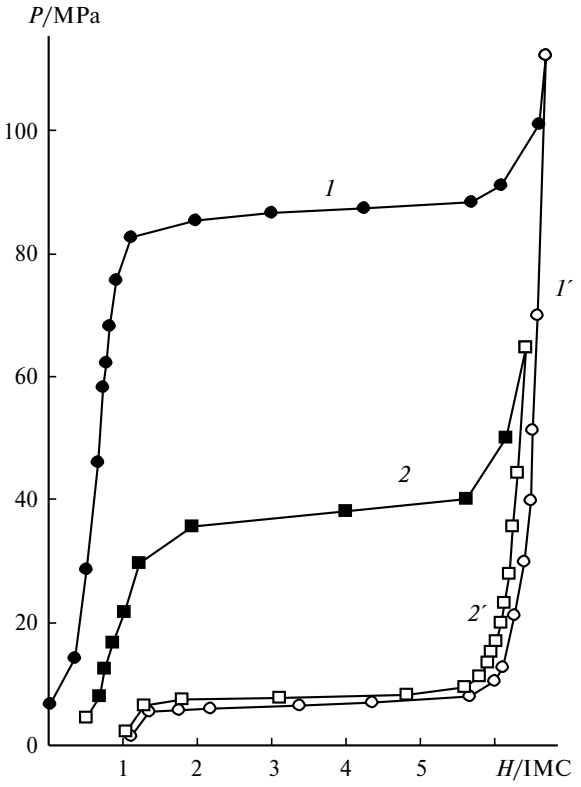

Fig. 3. Hydrogen absorption (*1*, *2*) and desorption (*1′*, *2′*) isotherms in the $CeNi_5$—H_2 system at 295 K: *1*, *1′*, 1st cycle and *2*, *2′*, 3rd cycle.

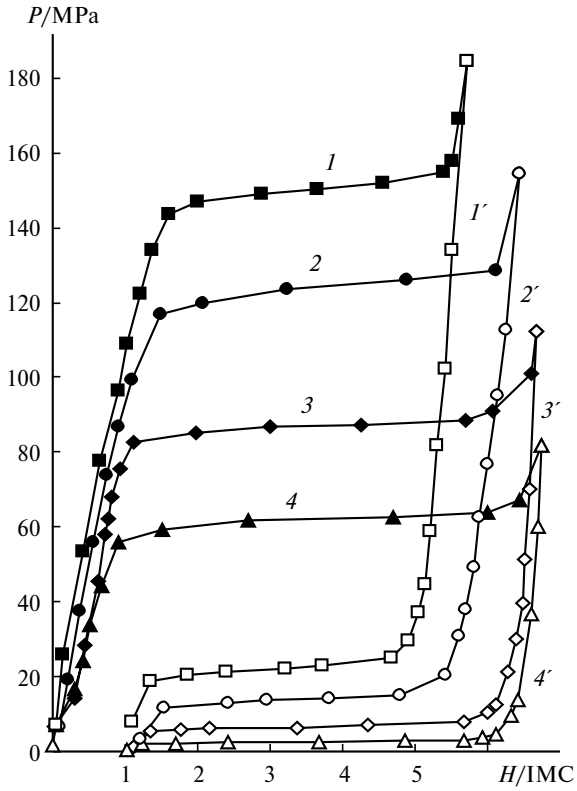

Fig. 4. Hydrogen absorption (*1*—*4*) and desorption (*1′*—*4′*) isotherms of the 1st cycle in the $CeNi_5$—H_2 system at different temperatures: 273 (*1*, *1′*); 295 (*2*, *2′*), 323 (*3*, *3′*), and 343 (*4*, *4′*).

previously[16] been shown that the results of the third cycle are completely reproducible on the further multiple cycling. A comparison of the presented results with the data in Table 2 for $LaNi_5$ indicates a remarkable difference between the absolute ΔH values and ΔH for the hysteresis. This specific feature is related to a lower thermal stability of β-hydride of $CeNi_5$ compared to $LaNi_5$ β-hydride, as known from literature. A more pronounced decrease in ΔH_{des} during activation for $CeNi_5$ also should be mentioned.

The results obtained in this work can be summarized as follows.

The first absorption—desorption cycle in the $LaNi_5$—H_2 and $CeNi_5$—H_2 systems is characterized by reproducible values of the absorption capacity, equilibrium pressure, and hysteresis.

Table 3. Thermodynamic parameters for the $CeNi_5$—H_2 systems at 295 K

Cycle	p_{abs}	p_{des}	$RT\ln(f_{abs}/f_{des})$	ΔH_{abs}	ΔH_{des}
	MPa		kJ (mol^{-1} H_2)		
1	152	6.5	7.7	−14.6±0.4	25.7±1.1
3	29	7.5	3.3	−17.0±0.6	22.2±0.1

Analysis of the profiles of the heat release curves made it possible to observe an unusual effect of maximum splitting in the two-phase region at the first cycle of hydrogenation—dehydrogenation, which indicates a change in the reaction mechanism during activation.

The enthalpies of the $\alpha \rightarrow \beta$ phase transition for the first absorption—desorption cycle in the $LaNi_5$—H_2 system determined by the Tian—Calvet calorimetry and those calculated from the temperature plot of the equilibrium pressures of the $\alpha \rightarrow \beta$ phase transition for the first absorption—desorption cycle in the $CeNi_5$—H_2 system differ significantly from the corresponding thermodynamic functions of the completely activated systems.

At the same time, the general character of changing the thermodynamic parameters on going from the first cycle to the activated state is similar for both systems studied.

This work was financially supported by the Russian Foundation for Basic Research (Project No. 03-03-32992).

References

1. L. Belkbir, E. Joly, N. Gerard, T. C. Achard, and A. Percheron-Guegan, *J. Less-Common Met.*, 1980, **73**, 69.

2. J.-M. Joubert, M. Latroche, R. Gerny, A. Percheron-Guegan, and K. Yvon, *J. Alloys Comp*., 2002, **330—332**, 208.
3. M. P. Pitt, E. A. MacGray, E. H. Kisi, and B. A. Hunter, *J. Alloys Comp*., 1999, **293—295**, 118.
4. H. Inui, T. Yamamoto, M. Hirota, and M. Yamaguchi, *J. Alloys Comp*., 2002, **330—332**, 117.
5. E. A. MacGray, C. E. Buckley, and E. H. Kisi, *J. Alloys Comp*., 1994, **215**, 201.
6. M. P. Pitt, E. A. MacGray, and B. A. Hunter, *J. Alloys Comp*., 2002, **330—332**, 241.
7. R. A. Sirotina, A. P. Savchenkova, V. V. Burnasheva, I. F. Belyaeva, and K. N. Semenenko, *Zh. Obshch. Khim.*, 1988, **58**, 2526 [*J. Gen. Chem., USSR*, 1988, **58** (Engl. Transl.)].
8. N. A. Yakovleva, E. A. Ganich, T. N. Rumyantseva, and K. N. Semenenko, *J. Alloys Comp*., 1996, **241**, 112.
9. E. A. Ganich, N. A. Yakovleva, and K. N. Semenenko, *Izv. Akad. Nauk, Ser. Khim*., 1999, 21 [*Russ. Chem. Bull.*, 1999, **48**, 21 (Engl. Transl.)].
10. S. N. Klyamkin and V. N. Verbetsky, *J. Alloys Comp*., 1993, **194**, 41.
11. H. Hemmes, A. Driessen, and R. Griessen, *J. Phys. Chem.: Solid State Phys*., 1986, **19**, 9571.
12. X.-L. Wang and S. Suda, *Int. J. Hydrogen Enerdgy*, 1990, **15**, 569.
13. K. N. Semenenko, N. A. Yakovleva, and V. V. Burnasheva, *Zh. Obshch. Khim.*, 1994, **64**, 529 [*Russ. J. Gen. Chem*., 1994, **64** (Engl. Transl.)].
14. J. J. Murray, M. L. Post, and J. B. Taylor, *J. Less-Common Met*., 1980, **73**, 33.
15. A. P. Savchenkova and K. N. Semenenko, *Izv. Akad. Nauk SSSR. Neorg. Mater.*, 1989, **25**, 1312 [*Inorg. Mater*., 1989, **25** (Engl. Transl.)].
16. S. N. Klyamkin, V. N. Verbetsky, and A. A. Karih, *J. Alloys Comp*., 1995, **231**, 479.

Received July 19, 2004;
in revised form December 28, 2004